oscillator circuits. For an inverter oscillator (Fig. 5), we coupled five inverters together, with the output voltage of one inverter providing the input for the following. If the initial input to the first inverter is 0 V ($-V_c$), then the output of the fifth will be $-V_c$ (0 V). Returning the output of the fifth inverter as the input for the first inverter causes all of the inverters to sequentially change logic state. Consequently, the circuit oscillates with a characteristic frequency f_{osc}. If all transistors are identical, f_{osc} is $\frac{1}{10}$ of the switching delay frequency of an individual inverter. In reality, f_{osc} is limited by the slowest gate. For pentacene ring oscillators, f_{osc} is in the range of 100 to 500 Hz, and for PTV ring oscillators, f_{osc} is in the range of 10 to 50 Hz. These values are dominated by the RC time constant of the channel resistance R of the load transistor (the nonswitching transistor), which is given by $R \approx L/\mu WC_{ins}V_d$, and the channel capacitance C, which is given by $C = LWC_{ins}$, where C_{ins} is the capacitance per unit area of the insulator. During the oscillations, the drain bias V_d of the load transistor constantly varies between 0 V and $-V_c$, and thus, the channel resistance also varies. The measured frequencies are thus as expected, being lower but within an order of magnitude of the maximum transit frequency for a carrier between the source and drain contacts of a MISFET, $f_{transit} \approx \mu V_c/L^2$. Because mobilities as high as 0.1 cm^2 V^{-1} s^{-1} have been reported (1, 2), switching frequencies as high as 50 kHz are to be expected. More complicated NOR gate oscillators have also been successfully constructed. Here, in each of the NOR gates, one of the two inputs is held at 0 V, while the other input is provided by the output of the previous gate.

The observation of ring oscillations indicates that there is good reproducibility of the transistors, because each ring oscillator requires that all 10 transistors operate within given specifications. Devices are measured in air without encapsulation. A pentacene oscillator operating at 130 Hz has been observed to oscillate continuously for 24 hours, which represents in excess of 10^7 switching operations. Shelf lifetimes of both pentacene and PTV devices are at least an order of magnitude longer.

Through-conjugated polymers are thus suitable as the active semiconductor in cheap integrated electronic circuits. In order to replace the silicon-based substrates of this study and successfully produce electronic circuits by printing techniques, attention must now be directed toward the reliable printing of micrometer-scale conducting tracks.

REFERENCES AND NOTES

1. H. Fuchigami, A. Tsumura, H. Koezuka, *Appl. Phys. Lett.* **63**, 1372 (1993).
2. F. Garnier, R. Hajlaoui, A. Yassar, P. Srivastava, *Sci-ence* **265**, 1684 (1994).
3. A. Dodabalapur, L. Torsi, H. E. Katz, *ibid.* **268**, 270 (1995).
4. A. Bonnoit and R. Kielbasa, *L'Onde Électrique* **74**, 18 (1994).
5. G. Horowitz et al., *Synth. Met.* **54**, 435 (1993).
6. J. H. Burroughes, C. A. Jones, R. H. Friend, *Nature* **355**, 137 (1988).
7. P. Herwig, thesis, University of Mainz (1993).
8. I. Murase, T. Ohnishi, T. Noguchi, M. Hirooka, *Polym. Commun.* **28**, 229 (1987).
9. G. Horowitz, R. Hajlaoui, P. Delannoy, *J. Phys. III Paris* **5**, 335 (1995).
10. A. R. Brown, D. M. de Leeuw, E. E. Havinga, A. Pomp, *Synth. Met.* **68**, 65 (1994).
11. M. J. Powell et al., *Phys. Rev. B* **45**, 4160 (1992).
12. We thank P. Herwig and K. Müllen for providing the pentacene precursor and R. J. C. E. Demandt for synthesizing the PTV precursor. We thank J. F. C. Verhoeven, E. M. L. Alexander, and H. G. R. Maas for technical advice and support. Financial support is gratefully acknowledged from the European Economic Community under Esprit Program 7282 TOPFIT.

Optical Microfabrication of Chalcogenide Glasses

H. Hisakuni and K. Tanaka*

It was found that chalcogenide glasses can be shaped by stressing the glass under light illumination because light illumination enhances the fluidity of the glass. The mechanism of photoinduced fluidity was found to be photoelectronic, that is, athermal. The process can be applied to microfabrication of optical fibers and glassy films with a typical dimension of 10 to 100 micrometers.

Unlike crystalline materials, glass can be shaped into arbitrary forms at supercooled states. In the supercooled state, glass has a viscosity of less than $\sim 10^{13}$ poise (1–3) and has moderate fluidity. Such a fluid state can be attained by heating a glass above the glass transition temperature (1–3). Here, we demonstrate that the fluid state can be obtained by an athermal process, through illumination with visible light. We have observed photoinduced fluidity in several kinds of chalcogenide glasses and describe here the characteristics of a representative chalcogenide glass As$_2$S$_3$ (2, 4) in a photoinduced fluid state.

Optically processed As$_2$S$_3$ glass is shown in Fig. 1. In Fig. 1A, the sample is 50 μm in thickness and approximately 0.2 mm by 2 mm in lateral dimension. The sample was prepared through vacuum evaporation and then annealed at the glass transition temperature ($\sim$450 K), a process commonly used for stabilizing glass structures (2). Next, one end of the sample was pasted to a glass slide, and the other end was bent with a stick. We confirmed that the bending was elastic because the deformed glass recovered when the stress was removed. However, when the bent glass flake was illuminated locally by focused light, permanent deformation occurred (Fig. 1A). The illuminated part, indicated by an arrow in the figure, becomes viscous, and the sample is bent segmentally. In Fig. 1B, an As$_2$S$_3$ optical fiber with a diameter of 100 μm was illuminated with focused light and subject-

---
Department of Applied Physics, Faculty of Engineering, Hokkaido University, Sapporo 060, Japan.

*To whom correspondence should be addressed.

ed to elongated stress. Only the illuminated position becomes viscous, and as a result, it becomes constricted. In these two examples, we see that the deformations are restricted to a scale of $\sim$100 μm, which corresponds to the focused light spot. Such local deformations of glasses may be very difficult to achieve with thermal techniques (2, 5) because of heat conduction.

To understand the mechanism of photoinduced fluidity, we measured the fluidity (the inverse of the viscosity) in As$_2$S$_3$ glass under illumination. The fluidity was evaluated through a creep measurement (2, 6). A typical result is shown in Fig. 2. In the dark no appreciable elongation occurred, but under illumination from a He-Ne laser, the length of the flake increased dramatically.

The viscosity η can be defined as
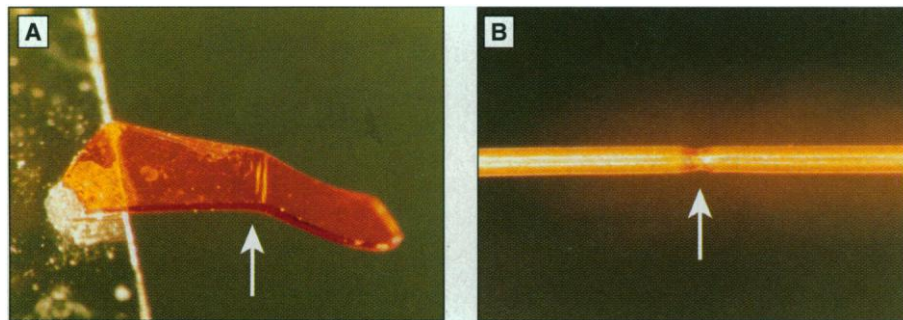
$$de/dt = \tau/\eta \qquad (1)$$

where e is the viscous strain and τ is the stress (2, 6). Using this equation, we calculate that $\eta \geq 10^{14}$ poise in the dark and $\eta \approx 5 \times 10^{12}$ poise under illumination. This viscosity value is consistent with the deformation shown in Fig. 1. We also confirmed that the viscosity decreases with increasing light intensity.

The temperature dependence of the viscosity of As$_2$S$_3$ is shown in Fig. 3. In the dark at approximately room temperature, the viscosity of As$_2$S$_3$ flakes cannot be measured, which means that $\eta \geq 10^{14}$ poise. In contrast, the viscosity of the illuminated sample increases at higher temperatures, that is, the photoinduced fluidity becomes less appreciable at higher temperatures.

The temperature dependence shown in Fig. 3 strongly suggests that the photoin-

Fig. 1. Optically processed As_2S_3. (**A**) An As_2S_3 flake was subjected to bending stress and illuminated through a side surface (indicated by the arrow) with a focused beam emitted from a 10-mW He-Ne laser for 2 hours. (**B**) An As_2S_3 optical fiber was illuminated with the He-Ne laser light for 5 hours under elongating stress.

under which this phenomenon occurs are as follows: (i) The glass must be optically excited with light of $\hbar\omega \lesssim E_g$, where E_g is the bandgap energy of a material of interest. In the present demonstration, $E_g \simeq 2.4$ eV and $\hbar\omega \simeq 2.0$ eV. If $\hbar\omega \geq E_g$, although electrons and holes can be excited more efficiently, the excitation occurs only in a surface region because the penetration depth of bandgap light is typically 1 μm (2). In that case, optical fabrication may be possible only in thin (~1-μm thick) films, and such films will not be practically useful. (ii) It seems necessary that excited carriers recombine, accompanying the bond ruptures as described above. In this respect, the chalcogenide glass, which has a low coordination number of atoms, may be preferred (2, 4, 9).

In conclusion, it is known that chalcogenide glasses exhibit a variety of photoinduced phenomena at the microscopic scale (12), but our study demonstrates a phenomenon at the macroscopic scale. That enhanced fluidity occurs under light illumination indicates that the glass transition can be induced through photoelectronic excitation, a process needing further study. Photoinduced fluidity could have many applications, including applications in casting processes. Chalcogenide glasses are currently used as optical components, such as passive and active optical fibers in the infrared region (13, 14). The method presented here will be especially suitable to the production of micro-optic components (7), as it provides a way to bend plastically optical fibers on a small scale, a capability that also holds promise for the fabrication of integrated fiber circuits.

duced fluidity is not governed by the temperature rising as a result of light absorption. If the temperature rise governed the fluidity enhancement, we might assume that the fluidity induced by illumination would increase with temperature, because the fluidity in the dark increases with temperature (2, 3), and the light-induced temperature rise would be mostly constant at all temperatures (7). However, the experimental result is contrary to this prediction. In addition, it is known that the absorption coefficient of As_2S_3 at a wavelength of 633 nm (photon energy, $\hbar\omega$, is 2.0 eV) is small, ~1 cm^{-1} (2), and accordingly, the temperature rise under the present experimental situation is estimated to be less than ~0.1 K (7), which cannot exert substantial changes in the fluidity.

Alternatively, the temperature dependence implies that photoinduced fluidity is caused by a photoelectronic process. It has been demonstrated through photoconduction experiments that illumination can excite electrons and holes (8). When the excited carriers geminately recombine, some transformation of atomic bonds may

occur, which releases the applied stresses. If a sample is illuminated at a high temperature, the excited carriers may diffuse without recombining geminately. Accordingly, the photoinduced fluidity will decrease at higher temperatures.

The atomic change, however, is largely speculative at present, because the amorphous structure itself has not yet been elucidated (2, 4, 9). There may be at least two possibilities. One is the interchange of covalent (intramolecular) bonds, which can be mediated by bond rupture and rebonding. Defective structures may play a certain role in the process (10). The other is the weakening of intermolecular bonds. Ihm proposed that in chalcogenide glasses, layerlike clusters are "buckled" at some atoms (11). If the atoms buckling the layerlike clusters are optically excited, the clusters are likely to slip past each other, which may also be effective in releasing applied stresses.

At present, it is not known whether photoinduced fluidity is inherent to chalcogenide glasses or if it also occurs in other amorphous materials such as oxide glasses and organic polymers. Some conditions

REFERENCES AND NOTES

1. W. Kauzmann, *Chem. Rev.* **43**, 219 (1948).
2. J. Zarzycki, Ed., *Materials Science and Technology* (VCH, Weinheim, Germany, 1991), vol. 9.
3. C. A. Angell, *Science* **267**, 1924 (1995).
4. J. C. Phillips, *Phys. Today* (27 February 1982); *J. Non-Cryst. Solids* **34**, 153 (1979).
5. C. D. Poole, H. M. Presby, J. P. Meester, *Electron. Lett.* **30**, 1437 (1994).
6. J. D. Ferry, *Viscoelastic Properties of Polymers* (Wiley, New York, 1970).
7. H. Hisakuni and K. Tanaka, *Appl. Phys. Lett.* **65**, 2925 (1994).
8. _____, unpublished results.
9. S. R. Elliott, *Nature* **354**, 445 (1991).
10. H. Koseki and A. Odajima, *Jpn. J. Appl. Phys.* **21**, 424 (1982).
11. J. Ihm, *J. Phys. C.* **18**, 4741 (1985).
12. K. Tanaka, *Rev. Solid State Sci.* **4**, 511 (1990).
13. J. S. Sanghera, L. E. Busse, I. D. Aggarwal, *J. Appl. Phys.* **75**, 4885 (1994).
14. Y. Ohishi, A. Mori, T. Kanamori, K. Fujiura, S. Sudo, *Appl. Phys. Lett.* **65**, 13 (1994).
15. K. J. Habell and A. Cox, *Engineering Optics 343* (Pitman, London, 1966).
16. C. A. Angell, *J. Non-Cryst. Solids* **102**, 205 (1988).
17. We thank NTT Laboratory, Showa Electric Wire and Cable Company Limited, and Hitachi Microcomputer Engineering Limited for assistance with experiments.
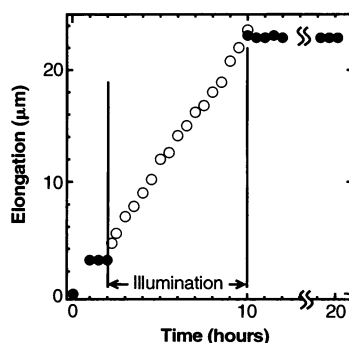
Fig. 2. Elongation of an As_2S_3 flake in the dark (solid circles) and under illumination (open circles). In this experiment, an As_2S_3 flake with a dimension of about 50 μm by 0.2 mm by 2 mm was pulled along the longest side length under a stress of 4.4×10^7 dyn/cm^2, and the elongation was measured in situ with an optical lever technique (15).
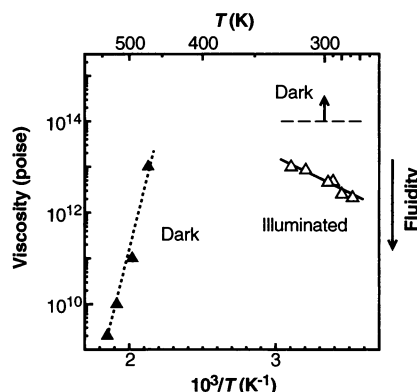
Fig. 3. Temperature dependence of the viscosity in As_2S_3 in the dark (greater than the dashed line) and under illumination (open triangles). The results were obtained from experiments of Fig. 2 at several temperatures. The high temperature data (solid triangles) obtained in supercooled As_2S_3 is cited from (16).